Heliyon 11 (2025) e44182

Contents lists available at ScienceDirect

Heliyon

journal homepage: www.cell.com/heliyon

Research article

The relationship of *IL-10* polymorphisms and brucellosis resistance in Mediterranean water buffalo

Andrea Fulgione [a,1], Antonio Gentile [a,1], Valentina Iovane [a], Francesca Paola Nocera [b], Maria Luisa Varricchio [a], Rosanna Capparelli [a,*]

[a] *Department of Agricultural Sciences, University of Naples Federico II, Piazza Carlo di Borbone 1, Portici, 80055, Naples, Italy*
[b] *Department of Veterinary Medicine and Animal Production, University of Naples Federico II, Via F. Delpino 1, 80137, Naples, Italy*

ARTICLE INFO

Keywords:
Interleukin-10
Brucella abortus
In silico study
Polymorphism
Association study

ABSTRACT

Interleukin-10 (IL-10) is one of the key anti-inflammatory cytokines produced during infections to suppress inflammation and to limit host tissue damages. However, some Gram-negative bacteria, like *Brucella abortus* (*B. abortus*), use IL-10 for neutralizing the host defensive mechanisms thus surviving within the host cells. Polymorphisms in the *IL-10* gene may affect the structure of the resulting protein and consequently its interaction with the proper IL-10 receptor (IL-10R), thus potentially compromising the inflammatory pathway triggered by pathogens such as *B. abortus*.

This study aimed to assess the relationship between *IL-10* polymorphisms and brucellosis using a combined methodology: *in silico* analyses (i.e. docking and Molecular Dynamic Simulations) - for predicting the protein modifications induced by single nucleotide polymorphisms (SNPs) - and association study.

The predictive analysis evidenced that the substitution of Threonine at position 175 with Methionine in the IL-10 protein sequence, may affect the IL-10/IL-10R interaction, while the genotyping analysis revealed that the g.4002T allele - resulting in the T175M substitution - is associated with resistance to brucellosis (OR = 0.45; p-value = 0.015), thus supporting the computational predictions.

This study suggests that the identified genetic variant alters the IL-10 structure and its interaction with the receptor, which may contribute to increase resistance to brucellosis, ultimately favouring pathogen clearance. The proposed approach could represent an alternative strategy for livestock disease management and control.

1. Introduction

Interleukin-10 (IL-10) is a key anti-inflammatory cytokine produced by host immune cells during infections to limit tissue damage and to ensure the pathogens clearance by modulating the immune response [1,2]. IL-10 elicits its function by interacting with the heterotetrameric IL-10 receptor complex (IL-10R) constituted by two IL-10R-alpha (IL-10RA) and two IL-10R-beta (IL-10RB) subunits. Upon IL-10 binding, the IL-10/IL-10RA complex interacts with IL-10RB, activating the Janus kinase 1 (Jak1) and Tyrosine kinase 2 (Tyk2) [3]. This activation triggers a signalling cascade that ends with Signal Transducer and Activator of Transcription 3 (STAT3)

* Corresponding author.
E-mail address: capparel@unina.it (R. Capparelli).
[1] These authors contributed equally to this work.

https://doi.org/10.1016/j.heliyon.2025.e44182
Received 9 August 2024; Received in revised form 9 October 2025; Accepted 11 November 2025
Available online 22 November 2025

phosphorylation, dimerization, and its translocation into the nucleus [4]. Here, STAT3 induces the transcription of Suppressor of Cytokine Signaling 3 (SOCS3), able to suppress the Mitogen-Activated Protein Kinase (MAPK) and Nuclear Factor kappa-light-chain-enhancer of activated B cells (NF-kB) activation, thereby inhibiting pro-inflammatory cytokine signalling and preventing an excessive inflammation [5]. This biological process highlights that IL-10 is important for controlling the excessive inflammatory response and favouring the host survival [6].

However, IL-10 can also exert a negative effect on the host immune response [7]. Some bacteria, like the intracellular *Brucella abortus* (*B. abortus*), have developed strategies to benefit from the host immune-regulatory mechanisms and establish a chronic infection.

B. abortus is a Gram-negative bacterium able to induce IL-10 production for neutralizing the host defensive mechanisms thus surviving within the immune cells. Specifically, the production of IL-10 down-regulates the T helper 1 (Th1) cell response and suppresses the Interferon gamma (IFN-γ) production through the inhibition of macrophage functions, thus favouring the bacterial survival within phagocytic cells [8–10]. Consistent with these findings, IL-10 neutralization was found to up-regulate the level of IFN-γ, as well as other pro-inflammatory cytokines, including Tumor Necrosis Factor beta (TNF-β), Interleukin-12 (IL-12) and Interleukin-6 (IL-6), in mice infected with *B. abortus*, thus decreasing the bacterial load and increasing the tissue damage [1,9].

Different studies have demonstrated that the presence of polymorphisms in *IL-10* gene could influence the development of brucellosis [8,11,12]. Given the significant impact of brucellosis on human health and livestock [13–15] such as abortion, reduced milk production and significant economic losses for disease management [16–18], investigating and better understand the host defensive mechanisms is necessary. Despite various attempts to limit the spread of infection, brucellosis remains endemic in several geographical areas such as South America countries and Mediterranean Europe [19,20].

This study aims to investigate the relationship between *IL-10* polymorphisms and brucellosis through integrated methodologies, including *in silico* approaches like docking and Molecular Dynamic Simulations (MDS), and association study. This combined approach could provide evidence about the possible association between *IL-10* genetic variations and brucellosis susceptibility.

2. Materials and methods

2.1. Sampling

DNA samples were extracted from the peripheral blood of 192 Italian Mediterranean Buffaloes raised in three herds located in the province of Caserta (Campania region, Italy) and enrolled in a previous study [21]. All the herds were in the same geographical area and managed under comparable extensive systems, with similar environmental conditions, brucellosis prevalence and management practices.

The animals were grouped in positive (infected) and negative (uninfected) to *B. abortus* infection, according to the official test (buffered Brucella antigen test and complement fixation test), as reported by the ANNEX III of the EU Regulation 2020/689 [22]. For this study, 96 DNA samples were selected for each group (i.e. 96 infected and 96 uninfected animals). This sampling was carried out according to a non-probability sampling method, from November 2022 to September 2023. All the animals enrolled for this study were lactating buffaloes between 40 and 90 months of age and were from the same source population; by this way the uninfected had the same possibility as infected of becoming positive to brucellosis.

2.2. Primer design and sequencing analysis

The end-point PCR and sequencing analysis was carried out on 30 Mediterranean river buffaloes (15 brucellosis-positive and 15 negative). In order to identify possible Single Nucleotide Polymorphisms (SNPs) in the exon 5, the primer pairs design was carried out in a region including also part of the intron 4 and 5′ UTR region of the Mediterranean Water Buffalo *IL-10* (b*IL-10*) (GenBank assembly: GCA_000471725.1; NW_005783511.1:356114–360857; Gene ID: 102400790), using Benchling on-line software (https://www.benchling.com). The primer sequences were Fw: 5′-AGGTCCAGGGCAACACATAG-3′ and Rw: 5′-TCTAGGGGAGAGGCACAGTA-3’ (Supplementary Fig. S1). The PCR reaction mix included 200 ng of genomic DNA, 3 mM $MgCl_2$, 200 nmol of each primer, dNTPs each at 400 μM, 0.5 U of Taq DNA Polymerase (all from Promega). The thermal protocol consisted in 1 cycle at 95 °C for 5 min; 35 cycles at 94 °C for 1 min, 57.5 °C for 1 min and 72 °C for 45 s and a final cycle at 94 °C for 1 min, 65.0 °C for 1 min and 72 °C for 5 min. All PCR products were analysed directly by electrophoresis in 1.5 % agarose gel (Bio-Rad, Hercules, CA, USA) in 0.5X TBE (Tris-Borate-EDTA) buffer, stained with Safe View Classic (ABM's Safe View Classic). The expected amplicon size was 422 bp. The PCR products were purified and sequenced in outsourcing on both strands by CEINGE Institute.

2.3. bIL-10/IL-10R complex homology modelling

The Mediterranean Water Buffalo protein IL-10 (bIL-10) and its receptor (bIL-10R) were developed by adopting as model the human IL-10 (PDB_ID: 2ilk.1) and the human IL-10 complexed with the soluble IL-10R (PDB_ID: 1Y6K), respectively. The homology modelling was performed by using the Swiss Model web tool (https://swissmodel.expasy.org/). After its modelling, the bIL10 was superposed to the 1Y6K model, which contains both the ligand and its receptor, for reconstructing the complex bIL-10/bIL-10R. The quality of the complex was assessed by the following parameters: Ramachandran plot, normalized Qualitative Model Energy Analysis (QMEAN) Score, QMEAND global score, and Pro-Check tool. Chiron (https://dokhlab.med.psu.edu/chiron/login.php) and YASARA (http://www.yasara.org/minimizationserver.htm) web Servers [23] were then utilized to address the bIL-10 clashes and outliers thus

improving its structural integrity. Finally, the model was evaluated by MolProbity software (v. 4.5.2.).

2.4. Molecular Dynamic Simulations (MDS)

To better understand the effect of the amino acid substitutions (associated to the identified SNPs) on the binding affinity between bIL-10 and bIL-10R, the MDS analysis was performed by using GROMACS (version 2023.2) [21,24,25]. Briefly, the OPLS-AA (Optimized Potential for Liquid Simulation All-Atom) force field was applied to each atom of the complex [26,27] which was then solvated in a water-spaced box (model TIP3P). Ions were added to neutralize the charges, and the complex energy minimization was carried out to remove any steric clash.

The simulations run for 10 ns (ns) according to the following conditions: constant Boltzmann pressure (1 atm), temperature of 310 Kelvin (K), and a time step of 2 fs (fs). The stability of the complex over the entire simulation was evaluated by calculating the kinetic and energetic parameters. Specifically, the Root-mean-square deviation (RMSD) and Root-mean-square fluctuation (RMSF) were assessed to evaluate the structural changes and the amino acids flexibility of the complex, respectively; the Radius of Gyration (RoG) was instead adopted for estimating the complex compactness. Finally, the H-bonds number were analysed to determine the strength of interactions between the two proteins [25].

2.5. Solvent Accessible Surface Area (SASA) analysis

The SASA analysis was performed to investigate the intermolecular interactions and the effects of solvation in reference and mutagenized bIL-10/bIL-10R complexes [28,29]. It was calculated by using the Adaptive Poisson–Boltzmann Solver (APBS) Electrostatics plug-in of PyMOL software (v. 2.5.5) [30]. The analysis was carried out according to systems' default parameters (Amber force field; temperature at 310 K; solvent dielectric constant of 78.000 ε). The values were expressed between −5 and +5 kT/e.

2.6. Genotyping analysis

The genotyping analysis for the g.4002C>T polymorphism was carried out by an allele specific-PCR (AS-PCR). The reagents and concentrations were the same of the end-point PCR carried out for the exon 5 amplification and sequencing. However, the protocol was optimized based on the annealing temperatures of the primers used for genotyping (Table 1), which were previously reported by Iannaccone et al. [31].

2.7. Statistical analysis

Allele frequencies were calculated by simple allele counting [32]. The univariate logistic regression model was performed for estimating the association of b*IL-10* polymorphic sites with *B. abortus* infection. Odds ratio (OR) and 95 % confidence intervals were calculated by Fisher's exact test using the statistical package GraphPad Prism version 8 (GraphPad, La Jolla, CA, USA). The values were considered significant at p-value ≤ 0.05 [33].

3. Results and discussion

3.1. Sequencing and SNP identification

Thirty samples (15 infected and 15 uninfected animals) were randomly chosen and sequenced to identify possible SNPs in the exon 5 of b*IL-10* gene. The alignment of the sequencing results evidenced the presence of two SNPs in exon 5: g.3936G>A and g.4002C>T. These polymorphisms are responsible for the following amino acid substitutions in bIL-10 protein (UniProtKB ID: Q2PE56): p.Arg153Lys (R153K) and p.Thr175Met (T175M), respectively. The last polymorphism has been already identified in a previous work [31].

3.2. Homology modelling and 3D protein structure

The complex bIL-10/bIL-10R was constructed through homology modelling by using Swiss Model tool. Specifically, the bIL-10 component was developed by adopting the human IL-10 as reference structure, which showed an 80.89 % of sequence similarity

Table 1
List of the primers used for genotyping analysis.

Gene (SNP)	Primer	Primer sequence (5′-3′)	Amplicon size (bp)	Annealing Temperature
IL-10 (g.4002C>T)	Forward 1	TACATAGAAACCTACGTGACAA**C**	119	65.0 °C
	Forward 2	TACATAGAAACCTACGTGACAA**T**		
	Reverse	ATCGGATTTCAGAGGTCTTCCGT TTA		

Note. The alleles identified by AS-PCR forward primer are evidenced in bold character.

and 85.63 % of sequence coverage with the *Bubalus bubalis* homolog. The QMEAN global score of 0.73 ± 0.5 and a Ramachandran outlier of 1.11 % allowed us to select this model as the reference one (Fig. 1A and B).

The bIL-10R was instead modelled using the human IL-10R as template, which shows 70.95 % of sequence similarity and 39.40 % of sequence coverage (Fig. 1C and D). This low sequence coverage is due to X-ray crystallography limitations which cannot define the entire structure of proteins composed by intracellular and extracellular domains. Therefore, it was possible to develop only the extracellular domain of the bIL-10R through homology modelling. However, to perform an accurate analysis, the receptor needs to be bounded to the membrane; so, the protein transmembrane domain has been reconstructed *de novo* through Alpha-Fold2 and restrained to simulate the membranes bound. The developed model was shown in Fig. 2.

The models were optimized using Chiron and YASARA web servers which minimizes energy and solved clashes. The output models were then evaluated by MolProbity (vers. 4.5.2) which have provided the Ramachandran plot (Ramachandran outliers: 1.79 %), All Atom Clash score (2.36), Poor rotamers (1.44 %) and MolProbity score (1.73) (Supplementary Fig. S2).

3.3. MDS analyses

To evaluate the effects of the selected polymorphisms on the bIL-10 function, the reference type protein (WT) and the three mutagenized counterparts containing single substitution (i.e. R153K or T175M) or both (i.e. KM) were investigated by using GROMACS software (Fig. 3). Specifically, the RMSD, the RoG and the RMSF were evaluated. The RMSD of the complex evidenced that all the substitutions alone or in combination did not cause a significant shift from the reference complex (Fig. 3A). The RoG analysis, instead, highlighted a greater stability of WT and R153K complexes, respect to T175M and KM; thus, suggesting a better interaction between the bIL-10 and its specific receptor (Fig. 3B). Finally, the RMSF analysis of the bIL-10 displayed that the T175M substitution caused a marked reduction of amino acid fluctuation compared to the reference, indicating hindrance to their movement capability (Fig. 3C). In particular, the protein structure including the amino acids ranging from the positions 29 to 67 and those from 87 to 113, resulted to be particularly rigid. Furthermore, the amino acids from position 42 to 67 (constituting the bIL-10 external loop) are involved in the bIL-10/bIL-10R interaction and H-bonds network formation; by this way, a decreased movement flexibility could compromise the interaction with receptor, consistently with the RoG results. Therefore, the H-bond network analysis was carried out to verify the above hypothesis (Fig. 4). The result showed that the complex with the highest number of H-bonds during the simulation was

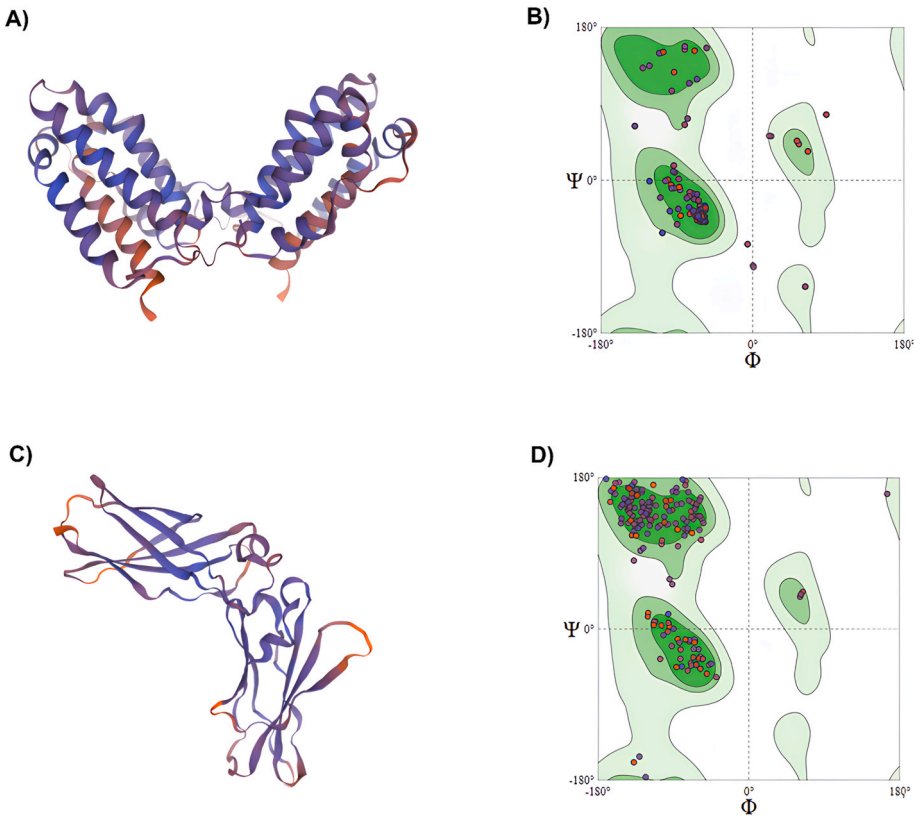

Fig. 1. bIL-10 and bIL-10R homology modelling. Homology modelling of the Mediterranean Water Buffalo IL-10 (bIL-10) and its receptor IL-10R (bIL-10R). 3D structure of A) bIL-10 and C) the bIL-10R (1B) modelled according to the human crystallographic structures 2ilk.1 and 1Y6K, respectively. Ramachandran plot of B) bIL-10 and D) bIL-10R. All bIL-10R amino acids are in their allowed Phi and Psi conformations (1D), while few amino acids of bIL-10 (4 out 385) do not fit with the expected conformation.

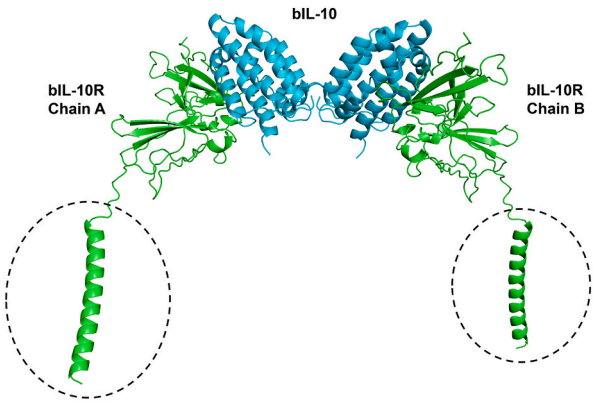

Fig. 2. bIL-10/bIL-10R complex 3D structure. bIL-10/bIL-10R complex obtained through homology modelling. bIL-10 is coloured in cyan while bIL-10R is in green. The trans-membrane domain of bIL-10R developed by ab initio prediction through AlphaFold are evidenced by dotted circles.

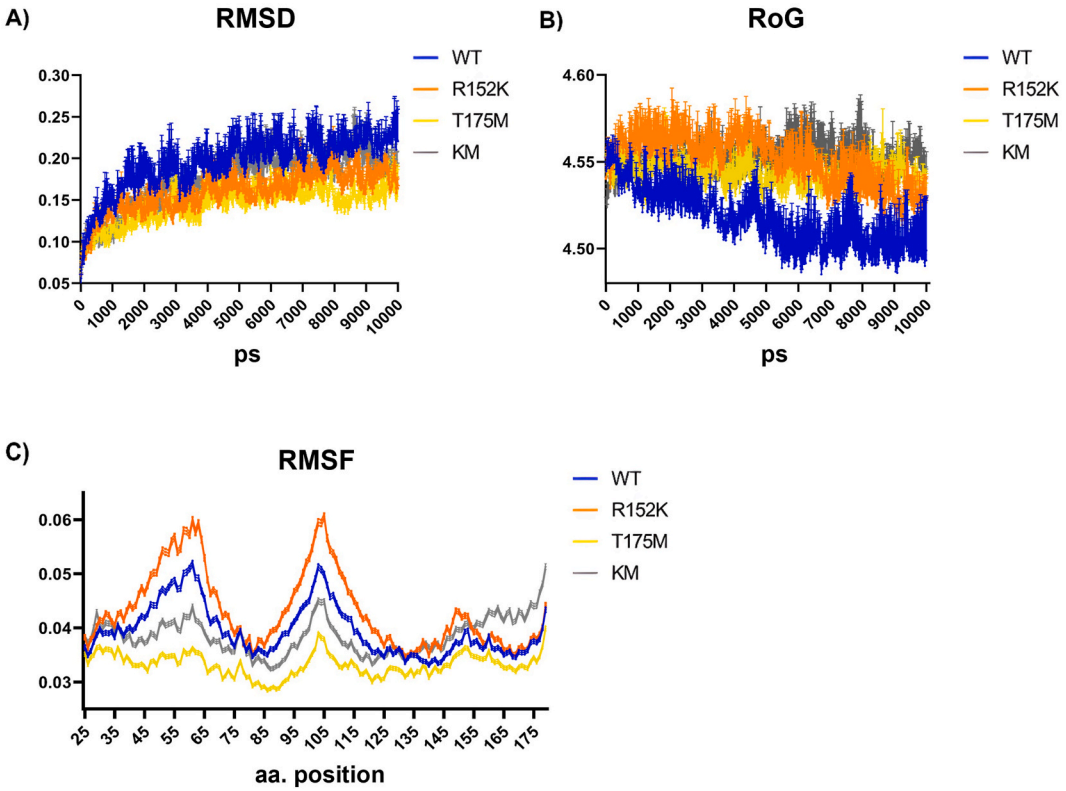

Fig. 3. MDS analysis of bIL-10/bIL-10R complex. A) RMSD analysis of the bIL-10/bIL-10R highlighting that the T175M is the complex which diverge more from the WT. B) RoG analysis which evaluate the stability of the globular form of the protein/receptor complex. This analysis evidences the WT as the most stable complex. C) RMSF analysis of the bIL-10 alone to investigate the effect of amino acids substitutions. The amino acids from position 29 to 67, are more flexible and dynamic in the WT and R153K complex respect to T175M.

the WT (19 ± 1.8) while the complex containing the Methionine at position 175 (T175M) was the one with the lowest H-bonds numbers (15 ± 2.0) (Fig. 4B). During the entire simulation time, it has been observed that the maximum number of H-bonds was at 5300 picoseconds (ps) in the WT complex, while the lowest number was at 2550 ps in the T175M complex (Fig. 4A). H-bonds differences between the WT and the mutagenized complexes were analysed by one-way ANOVA multiple comparison test which demonstrated a statistical significative difference between WT and T175M (p-value = 0.0019) (Fig. 4B). To deeply investigate the differences between the above two complexes, the MDS data were extracted at 2550 ps, 5300 ps, and 9100 ps to be further investigated (Supplementary Fig. S3).

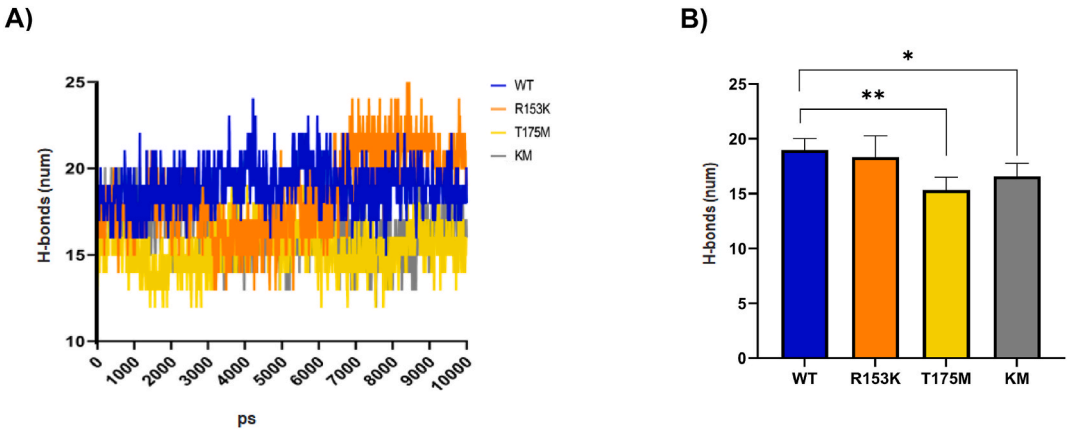

Fig. 4. H-bonds analysis. H-bonds analysis between bIL-10 and bIL-10R. A) H-bonds number over the 10 ns of simulation. The WT complex is the one showing the higher number of H-bonds, except for the last part of simulation. B) The same analysis is plotted as H-bond average. As represented, the WT complex have formed an average of 19 ± 1.8 H-bonds while the T175M formed 15 ± 2.0 H-bonds.

3.4. Structural and electrostatic analyses

The MDS analysis evidenced that the T175M substitution could reduce the motility of the amino acids involved in the interacting domains of bIL-10/bIL-10R, thus significantly reducing the number of H-bonds.

To better understand whether other variables could influence the number of H-bonds, the Solvent Accessible Surface Area (SASA) analysis was carried out for analysing WT and T175M complexes at 9100 ps, time at which RoG and H-bonds analyses evidenced a most

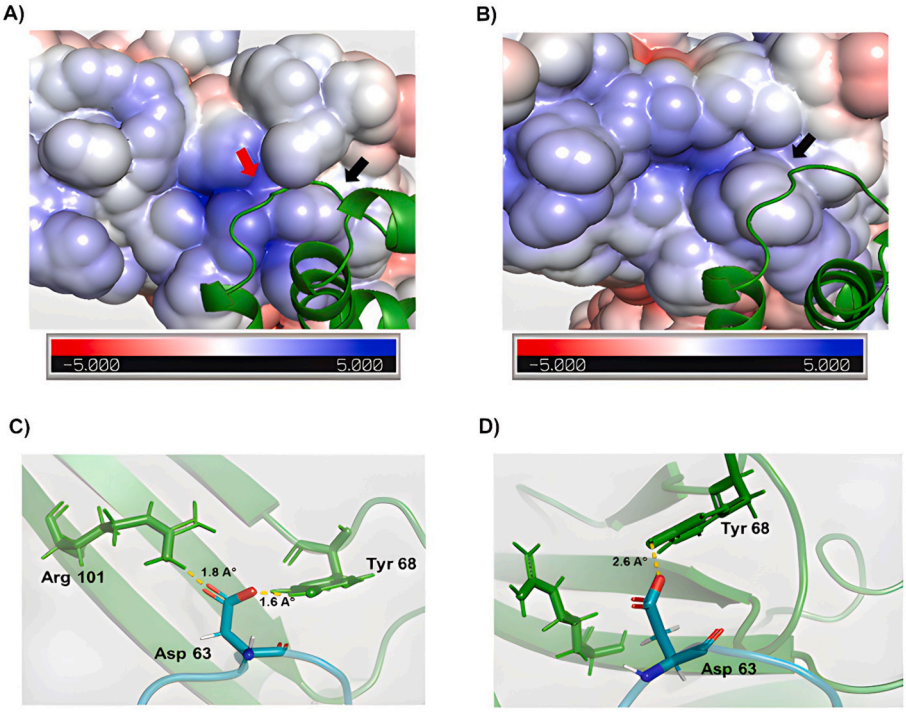

Fig. 5. WT and T175M APBS and H-bond network analyses. A) and B) shows the charges differences between WT and T175M complexes, respectively. As indicated by red arrow, there is a gain of positive charges in the WT complex respect to T175M. This loss positive charges in T175M could explain the detachment of the bIL-10 external loop (aa. 42–67), indicated by black arrow, from the positive binding pocket on the receptor bIL-10R. C and D deepen the H-bonds interactions between the bIL-10 (cyan) and the bIL-10R positive binding pocket (green). As shown in Fig. 5C, the Asp63 of WT strongly binds the Arg101 (1.8A°) and Tyr 68 (1.6A°) of bIL-10R. However, in T175M complex the H-bond network change and the Asp63-Tyr68 bond distance increase to 2.6A° while the Asp63-Arg101 bond is lost due to the increased distance between these two amino acids of 10.2A° (Supplementary Fig. S3).

Table 2
Association of the *IL-10* polymorphic site with *B. abortus* infection.

Genes (SNP)	Amino acid substitution	Status	Number of individuals in each genotype			Total	Total number of alleles		OR (CI)[a]	P-value
			CC	CT	TT		C	T		
IL-10 (g.4002C>T)	T175M	Infected	79	17	0	96	175	17	0.45 (0.24–0.83)	0.015
		Uninfected	65	28	3	96	158	34		

[a] CI (confidence intervals).

significant divergence between the two complexes. As shown in Fig. 5, the bIL-10R had a more positive charged area in the case of WT complex respect to the T175M. This positive charge was due to the presence of amino acids such as the Arg101 (Fig. 5A–C).

T175M (Fig. 5B–D) showed a reduction of positive charges in the same area (indicated by red arrow in Fig. 5A). Being the external bIL-10 loop highly negatively charged (Supplementary Fig. S4), the above reduction of positive charges in the bIL-10R could reduce the binding affinity between the receptor and its ligand. This, together with the RMSF analysis, which showed a movement reduction in the amino acids belonging to this loop (from 42 to 67), could explain the different behaviour when T175M substitution was present. By this way, the presence of this last substitution caused the bIL-10 shifting out from the binding pocket and an increase of H-bond distance between Asp63 and Tyr68 (from 1.6A° to 2.6A°) and the loss of the binding with the Arg101 (Fig. 5B–D).

Indeed, while the Asp63, in the case of WT complex, robustly binds the Arg101 (1.8A°), in the T175M this bond was lost due to the shift of the loop which drives away from the Arg101 up to 10.2A° (Supplementary Fig. S5E–F). The charge reduction was measured through ImageJ software, and it shifted from 1.84 Kt/e to 1.70 Kt/e (Supplementary Fig. S5C–D). This agrees with the reduction of the SASA from 1649.44 A^2 in the WT to 1472.97 A^2 in the T175M model (Supplementary Fig. S5A–B).

However, at the selected time of 9100 ps, the effects due to the T175M polymorphism were not limited to interval Asp63-Arg101. Indeed, while the WT complex formed 12 H-bonds between the bIL-10 and bIL-10R, the T175M complex had only 7 H-bonds. In addition to the Asp63-Arg101 bond loss, the T175M did not displayed the Gln69-Asn96; Gln69-Arg94; Glu170-Arg213 and Gln178-Asn164 bonds.

Overall, these results suggests that the amino acid substitution induced a change of the bIL-10/bIL-10R electrostatic surface, which leads to reduced interaction potential and a decreased solvent accessible area. This condition, associated to the low flexibility of protein structure including the amino acids between the positions 42 and 67, led to a worst positioning of this loop and finally to a weaker H-bonds network that negatively compromise the stability between the bIL-10/bIL-10R.

Based on the above *in silico* results, the association study was carried out only for the T175M polymorphism.

3.5. Association study

Referring to the T175M polymorphism, the AS-PCR analysis of the two groups (i.e. infected and uninfected animals) of Italian Mediterranean water Buffalo allowed us to identify the homozygous (CC or TT) and heterozygous (CT) conditions (Supplementary Fig. S6). The results evidenced the association of the g.4002T allele, resulting in the T175M substitution, with resistance to brucellosis (OR = 0.45; p-value = 0.015) (Table 2), thus providing additional elements for the *in silico* analysis. The results differed from those of Iannaccone et al. which have evidenced the linking between the same g.4002T allele and *Mycobacterium bovis* susceptibility [31]. Probably, the divergence of the results is due to the different type of bacteria (*B. abortus* is Gram negative while *Mycobacterium bovis* is Gram positive) and to the consequently mechanisms of inflammatory process activated by the above bacteria.

In fact, IL-10 can exert a different role during different infections. In some cases, higher IL-10 level can overcontrol the T-cell responses, thus inducing a chronic infection, while lower or no IL-10 expression could lead to a fatal host-mediated pathology. By this way, IL-10 can be considered as "essential" for balancing the host responses to all pathogens and the presence of polymorphisms on the gene could alter its expression thus influencing the resistance/susceptibility to a pathology [34].

Considering the resistance to a pathogen as multifactorial, we aim to evaluate if the presence of the g.4002T allele would be able to increase the brucellosis resistance detected in a previous study in Mediterranean Water Buffaloes having specific *TLR4* exon 3 polymorphisms [21]. The results have shown that the presence of g.4002T allele in animals having the resistance homozygous condition at specific polymorphic sites of the *TLR4* gene (i.e. AA for c.672A>C and GG for c.902G>C) was able to increase the brucellosis resistance in the same animals, giving an OR value of 0.18 but a p-value not statistically associated (i.e. 0.32). Probably, this last value is dependent from the limited number of samples enrolled for the study and consequently to the reduced number of animals having the selected alleles for the *TLR4* and *IL-10* genes. Further study needs to be carried out to better investigate this haplotype condition.

Our result also supports the hypothesis about the IL-10 involvement in brucellosis. In fact, although the IL-10 pathway activation is essential for the host survivor, some intracellular bacteria such as *B. abortus,* trigger the IL-10 production for suppressing the Th1 response and IFN-γ production, events able to compromise macrophage function and promote the bacterial survival within phagocytic cells [8–10].

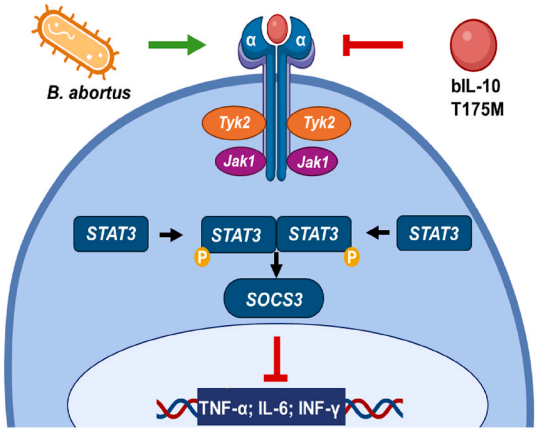

Fig. 6. IL-10 pathway. The IL-10 pathway starts with IL-10 binding to its receptor thus triggering a signalling cascade which causes nuclear translocation of STAT3, which in turn promotes the SOCS3 transcription. SOCS3 inhibits MAPK and NF-kB activation, thereby suppressing pro-inflammatory cytokine signalling and reducing inflammation, so favouring host survival. However, some bacteria like *Brucella* spp., can induce IL-10 production to suppress the Th1 response and IFN-γ production, hindering macrophage function and promoting bacterial survival within phagocytic cells. The presence of the T175M polymorphism can compromise the IL-10/IL-10R interaction thus preventing pathogens from exploiting the IL-10 pathway to evade the immune response.

4. Conclusions

The proposed approach combines *in silico* structural and electrostatic analyses with association studies to better understand the immune response triggered by pathogens such as *Brucella* spp. The study provides possible insights into the structural and functional implications of the T175M polymorphism in bIL-10 and about the interaction with its receptor bIL-10R. Specifically, the T175M substitution induces an increased rigidity of the amino acids involved in the interaction domain, a charge variation and a reduced number of hydrogen bonds, thus potentially compromising the interaction with its receptor.

The protective effect of T175M polymorphism can be understood through the role of IL-10 in the immune response. IL-10 is an anti-inflammatory cytokine that suppresses pro-inflammatory cytokine production and also limits the immune response activation (Fig. 6). During *B. abortus* infection, high levels of IL-10 can enhance bacterial survival by down-regulating the Th1 immune response, inhibiting macrophage function, and promoting a Th2-biased immune response. Our association study suggests that the g.4002T allele may have a protective role, thus supporting the hypothesis that a genetic variant - potentially altering IL-10 activity - might influence the immune balance, thereby contributing to a more effective immune response and increased resistance against brucellosis. The proposed approach could represent an alternative strategy for livestock disease management and control.

5. Limitation of the study

This study adopts the *in silico* analysis to predict the potential effects of *IL-10* SNPs on the structure and function of the IL-10 protein, as well as its interaction with the specific receptor IL-10R, in the context of buffalo brucellosis. While this approach provides useful preliminary insights into how genetic variations might influence protein-receptor binding, they are inherently limited by the predictive nature of the models used. The *in silico* analysis cannot fully replicate the complexity of biological environments, and the accuracy of the predictions depends on the quality of the structural data and algorithms applied. Moreover, the functional consequences of the identified SNPs on disease susceptibility remain speculative until validated through *in vitro* or *in vivo* experimental studies. Therefore, our findings should be interpreted cautiously, serving primarily as a foundation for further empirical research to clarify the role of *IL-10* variants in buffalo brucellosis. Further experimental studies involving a larger sample size and the evaluation of IL-10 transcription levels in both brucellosis-positive and -negative animals are needed to confirm the functional impact of the *IL-10* SNP on the inflammatory response.

CRediT authorship contribution statement

Andrea Fulgione: Writing – review & editing, Writing – original draft, Visualization, Project administration, Investigation, Formal analysis. **Antonio Gentile:** Writing – original draft, Visualization, Methodology, Data curation, Conceptualization. **Valentina Iovane:** Validation, Software, Formal analysis. **Francesca Paola Nocera:** Validation, Methodology. **Maria Luisa Varricchio:** Formal analysis. **Rosanna Capparelli:** Writing – review & editing, Visualization, Supervision, Resources, Project administration, Funding acquisition, Conceptualization.

Data availability statement

Data will be made available on request. For requesting data, please write to the corresponding author.

Ethics statement

Individual peripheral blood samples were collected during the routine prophylaxis of the farm by an official veterinarian of ASL (Local Sanitary Unit) of the Ministry of Health. For this reason, Animal Care and Use Committee approval was not necessary.

Funding

This work was supported by theMinistry of Universities and Research, Italy. (Project number PON01_00486 GENOBU).

Declaration of competing interest

The authors declare that they have no known competing financial interests or personal relationships that could have appeared to influence the work reported in this paper.

Appendix A. Supplementary data

Supplementary data to this article can be found online at https://doi.org/10.1016/j.heliyon.2025.e44182.

Abbreviations

Abbreviations	Definition
IL-10	Interleukin-10
B. abortus	*Brucella abortus*
IL-10R	IL-10 receptor
SNPs	Single Nucleotide Polymorphisms
IL-10RA	IL-10R-alpha
IL-10RB	IL-10R-beta
Jak1	Janus kinase 1
Tyk2	Tyrosine kinase 2
STAT3	Signal Transducer and Activator of Transcription 3
SOCS3	Suppressor of Cytokine Signaling 3
MAPK	Mitogen-Activated Protein Kinase
NF-kB	Nuclear Factor kappa-light-chain-enhancer of activated B cells
Th1	T helper 1
IFN-γ	Interferon gamma
TNF-β	Tumor Necrosis Factor beta
IL-12	Interleukin-12
IL-6	Interleukin-6
TBE	Tris-Borate-EDTA
bIL-10	Mediterranean water buffalo IL-10
bIL-10R	Mediterranean water buffalo IL-10 Receptor
MDS	Molecular Dynamic Simulations
OPLS-AA	Optimized Potential for Liquid Simulation All-Atom
QMEAN	Qualitative Model Energy ANalysis
ns	nanoseconds
fs	femtoseconds
K	Kelvin
RMSD	Root-mean-square deviation
RMSF	Root-mean-square fluctuation
RoG	Radius of Gyration
SASA	Solvent Accessible Surface Area
APBS	Adaptive Poisson–Boltzmann Solver
AS-PCR	Allele specific-PCR
OR	Odds ratio
ps	picoseconds

References

[1] H.F. Peñaloza, B.M. Schultz, P.A. Nieto, G.A. Salazar, I. Suazo, P.A. Gonzalez, C.A. Riedel, M.M. Alvarez-Lobos, A.M. Kalergis, S.M. Bueno, Opposing roles of IL-10 in acute bacterial infection, Cytokine Growth Factor Rev. 32 (2016) 17–30, https://doi.org/10.1016/J.CYTOGFR.2016.07.003.

[2] R.A. Saxton, K.C. Garcia, R.A. Saxton, K.C. Garcia, Cryo-EM structure of the IL-10 receptor complex provides a blueprint for ligand engineering, FEBS J. 289 (2022) 8032–8036, https://doi.org/10.1111/FEBS.16207.

[3] R. Verma, L. Balakrishnan, K. Sharma, A.A. Khan, J. Advani, H. Gowda, S.P. Tripathy, M. Suar, A. Pandey, S. Gandotra, T.S.K. Prasad, S. Shankar, A network map of Interleukin-10 signaling pathway, J. Cell Commun. Signal. 10 (2016) 61–67, https://doi.org/10.1007/S12079-015-0302-X.

[4] M. Saraiva, P. Vieira, A. O'Garra, Biology and therapeutic potential of interleukin-10, J. Exp. Med. 217 (2020), https://doi.org/10.1084/JEM.20190418/132577.

[5] V. Carlini, D.M. Noonan, E. Abdalalem, D. Goletti, C. Sansone, L. Calabrone, A. Albini, The multifaceted nature of IL-10: regulation, role in immunological homeostasis and its relevance to cancer, COVID-19 and post-COVID conditions, Front. Immunol. 14 (2023) 1161067, https://doi.org/10.3389/FIMMU.2023.1161067.

[6] K.N. Couper, D.G. Blount, E.M. Riley, IL-10: the master regulator of immunity to infection, J. Immunol. 180 (2008) 5771–5777, https://doi.org/10.4049/JIMMUNOL.180.9.5771.

[7] M.N. Xavier, M.G. Winter, A.M. Spees, K. Nguyen, V.L. Atluri, T.M.A. Silva, A.J. Bäumler, W. Müller, R.L. Santos, R.M. Tsolis, CD4+ T cell-derived IL-10 promotes Brucella abortus persistence via modulation of macrophage function, PLoS Pathog. 9 (2013), https://doi.org/10.1371/JOURNAL.PPAT.1003454.

[8] F. Budak, G. Göral, Y. Heper, E. Yilmaz, F. Aymak, B. Baştürk, O. Töre, B. Ener, H.B. Oral, IL-10 and IL-6 gene polymorphisms as potential host susceptibility factors in Brucellosis, Cytokine 38 (2007) 32–36, https://doi.org/10.1016/J.CYTO.2007.04.008.

[9] D.M. Fernandes, C.L. Baldwin, Interleukin-10 downregulates protective immunity to Brucella abortus, Infect. Immun. 63 (1995) 1130–1133, https://doi.org/10.1128/IAI.63.3.1130-1133.1995.

[10] S. Köhler, V. Foulongne, S. Ouahrani-Bettache, G. Bourg, J. Teyssier, M. Ramuz, J.P. Liautard, The analysis of the intramacrophagic virulome of Brucella suis deciphers the environment encountered by the pathogen inside the macrophage host cell, Proc. Natl. Acad. Sci. U. S. A. 99 (2002) 15711–15716, https://doi.org/10.1073/PNAS.232454299.

[11] X. Jin, S. Yin, Y. Zhang, Association between the IL-10-1082G/A, IL-10-819T/C and IL-10-592A/C polymorphisms and Brucellosis susceptibility: a meta-analysis, Epidemiol. Infect. 147 (2019), https://doi.org/10.1017/S0950268819002036.

[12] X. Jin, Y. Wu, S. Yin, X. Chen, Y. Zhang, Association between the IL-10 and IL-6 polymorphisms and brucellosis susceptibility: a meta-analysis, BMC Med. Genet. 21 (2020), https://doi.org/10.1186/S12881-020-01006-0.

[13] N.C. Hull, B.A. Schumaker, Comparisons of brucellosis between human and veterinary medicine, Infect. Ecol. Epidemiol. 8 (2018), https://doi.org/10.1080/20008686.2018.1500846.

[14] H.E. Mableson, A. Okello, K. Picozzi, S.C. Welburn, Neglected zoonotic diseases-the long and winding road to advocacy, PLoS Negl Trop Dis 8 (2014) e2800, https://doi.org/10.1371/journal.pntd.0002800.

[15] B. Ph, L. Hassan, S. Khairani-Bejo, M. Zainalabidin, The economic impact attributable to brucellosis among goat farms in Peninsula Malaysia and cost benefit analysis, Res. Opin. Anim. Vet. Sci. 5 (2015) 57–64. www.roavs.com. (Accessed 26 March 2024).

[16] M. Dadar, Y. Fakhri, Y. Shahali, A. Mousavi Khaneghah, Contamination of milk and dairy products by Brucella species: a global systematic review and meta-analysis, Food Res. Int. 128 (2020) 108775, https://doi.org/10.1016/J.FOODRES.2019.108775.

[17] K.A. Franc, R.C. Krecek, B.N. Häsler, A.M. Arenas-Gamboa, Brucellosis remains a neglected disease in the developing world: a call for interdisciplinary action, BMC Public Health 18 (2018) 1–9, https://doi.org/10.1186/S12889-017-5016-Y.

[18] M. Mellado, A.M. Garcia, B. Arellano-Reynoso, E. Diaz-Aparicio, J.E. Garcia, Milk yield and reproductive performance of brucellosis-vaccinated but seropositive Holstein cows, Trop. Anim. Health Prod. 46 (2014) 391–397, https://doi.org/10.1007/s11250-013-0502-4.

[19] M.L. Boschiroli, V. Foulongne, D. O'Callaghan, Brucellosis: a worldwide zoonosis, Curr. Opin. Microbiol. 4 (2001) 58–64, https://doi.org/10.1016/S1369-5274(00)00165-X.

[20] P. De Figueiredo, T.A. Ficht, A. Rice-Ficht, C.A. Rossetti, L.G. Adams, Pathogenesis and immunobiology of brucellosis: review of Brucella-host interactions, Am. J. Pathol. 185 (2015) 1505–1517, https://doi.org/10.1016/J.AJPATH.2015.03.003.

[21] A. Gentile, A. Fulgione, B. Auzino, V. Iovane, D. Gallo, R. Garramone, N. Iaccarino, A. Randazzo, G. Iovane, P. Cuomo, R. Capparelli, D. Iannelli, In vivo biological validation of in silico analysis: a novel approach for predicting the effects of TLR4 exon 3 polymorphisms on brucellosis, Infect. Genet. Evol. 118 (2024) 105552, https://doi.org/10.1016/J.MEEGID.2024.105552.

[22] Delegated regulation - 2020/689 - EN - EUR-Lex. https://eur-lex.europa.eu/eli/reg_del/2020/689/oj. (Accessed 3 July 2024).

[23] E. Krieger, K. Joo, J. Lee, J. Lee, S. Raman, J. Thompson, M. Tyka, D. Baker, K. Karplus, Improving physical realism, stereochemistry, and side-chain accuracy in homology modeling: four approaches that performed well in CASP8, proteins: structure, Function and Bioinformatics 77 (2009) 114–122, https://doi.org/10.1002/PROT.22570.

[24] M.J. Abraham, T. Murtola, R. Schulz, S. Páll, J.C. Smith, B. Hess, E. Lindah, GROMACS: high performance molecular simulations through multi-level parallelism from laptops to supercomputers, SoftwareX 1–2 (2015) 19–25, https://doi.org/10.1016/J.SOFTX.2015.06.001.

[25] S. Khan, U. Farooq, M. Kurnikova, Exploring protein stability by comparative molecular dynamics simulations of homologous hyperthermophilic, mesophilic, and psychrophilic proteins, J. Chem. Inf. Model. 56 (2016) 2129–2139, https://doi.org/10.1021/acs.jcim.6b00305.

[26] W.L. Jorgensen, D.S. Maxwell, J. Tirado-Rives, Development and testing of the OPLS all-atom force field on conformational energetics and properties of organic liquids, J. Am. Chem. Soc. 118 (1996) 11225–11236, https://doi.org/10.1021/JA9621760.

[27] G.A. Kaminski, R.A. Friesner, J. Tirado-Rives, W.L. Jorgensen, Evaluation and reparametrization of the OPLS-AA force field for proteins via comparison with accurate quantum chemical calculations on peptides, J. Phys. Chem. B 105 (2001) 6474–6487, https://doi.org/10.1021/JP003919D.

[28] P. Kumar, P.M. Dominiak, Combining molecular dynamic information and an aspherical-atom Data bank in the evaluation of the electrostatic interaction energy in multimeric protein-ligand complex: a case Study for HIV-1 protease, Molecules 2021 26 (2021) 3872, https://doi.org/10.3390/MOLECULES26133872.

[29] Z. Zhang, S. Witham, E. Alexov, On the role of electrostatics in protein–protein interactions, Phys. Biol. 8 (2011) 035001, https://doi.org/10.1088/1478-3975/8/3/035001.

[30] E. Jurrus, D. Engel, K. Star, K. Monson, J. Brandi, L.E. Felberg, D.H. Brookes, L. Wilson, J. Chen, K. Liles, M. Chun, P. Li, D.W. Gohara, T. Dolinsky, R. Konecny, D.R. Koes, J.E. Nielsen, T. Head-Gordon, W. Geng, R. Krasny, G.W. Wei, M.J. Holst, J.A. McCammon, N.A. Baker, Improvements to the APBS biomolecular solvation software suite, Protein Sci. 27 (2018) 112–128, https://doi.org/10.1002/PRO.3280.

[31] M. Iannaccone, G. Cosenza, A. Pauciullo, C. Martino, A. Ianni, R. Capparelli, G. Martino, Water buffalo (Bubalus bubalis) susceptibility to bovine tuberculosis is influenced by g.4002c>t polymorphism in interleukin-10 gene, Buffalo Bulletin 38 (2019) 135–139, https://doi.org/10.1080/1828051X.2019.1622269.

[32] D.S. Falconer, T.F.C. Mackay, Introduction to quantitative genetics, in: Trends in Genetics 12, fourth ed., 1996, p. 464. https://search.worldcat.org/title/422852955. (Accessed 3 July 2024).

[33] M.L. McHugh, The odds ratio: calculation, usage, and interpretation, Biochem. Med. 19 (2009) 120–126, https://doi.org/10.11613/BM.2009.011.

[34] P.S. Redford, P.J. Murray, A. O'Garra, The role of IL-10 in immune regulation during M. tuberculosis infection, Mucosal Immunol. 4 (2011) 261–270, https://doi.org/10.1038/MI.2011.7.